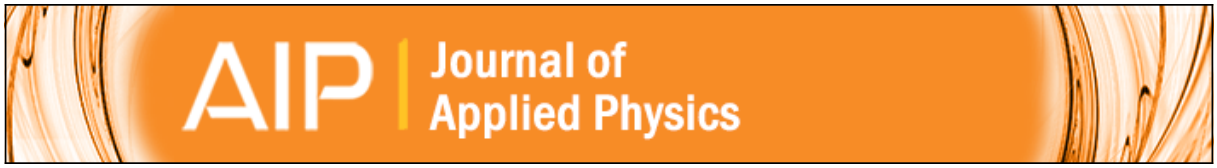

Si ion implantation-induced damage in fused silica probed by variable-energy positrons

A. P. Knights, P. J. Simpson, L. B. Allard, J. L. Brebner, and J. Albert

Citation: Journal of Applied Physics **79**, 9022 (1996); doi: 10.1063/1.362579
View online: http://dx.doi.org/10.1063/1.362579
View Table of Contents: http://scitation.aip.org/content/aip/journal/jap/79/12?ver=pdfcov
Published by the AIP Publishing

Si ion implantation-induced damage in fused silica probed by variable-energy positrons

A. P. Knights and P. J. Simpson
Department of Physics, The University of Western Ontario, London, Ontario, N6A 3K7 Canada

L. B. Allard and J. L. Brebner
Groupe de recherche en Physique et Technologie des Couches Minces, Département de Physique, Université de Montréal, Québec, H3C 3J7 Canada

J. Albert
Communications Research Center, P.O. Box 11490, Station H, Ottawa, Ontario, K2H 8S2 Canada

(Received 21 November 1995; accepted for publication 29 February 1996)

Samples of synthetic fused silica have been implanted at room temperature with silicon ions of energy 1.5 MeV. Fluences ranged from 10^{11} to 10^{13} cm^{-2}. Samples were probed using variable-energy positron annihilation spectroscopy. The Doppler-broadening S parameter corresponding to the implanted region decreased with increasing fluence and saturated at a fluence of 10^{13} cm^{-2}. It is shown that the decrease in the S parameter is due to the suppression of positronium (Ps) which is formed in the preimplanted material, due to the competing process of implantation-induced trapping of positrons. In order to satisfactorily model the positron data it was necessary to account for positron trapping due to defects created by both electronic and nuclear stopping of the implanted ions. Annealing of the 10^{13} cm^{-2} sample resulted in measurable recovery of the preimplanted S parameter spectrum at 350 °C and complete recovery to the preimplanted condition at 600 °C. Volume compaction was also observed after implantation. Upon annealing, the compaction was seen to decrease by 75%. © *1996 American Institute of Physics.* [S0021-8979(96)07811-5]

I. INTRODUCTION

Near-surface optical photosensitive waveguides can be created in fused silica substrates by subjecting them to high-energy ion irradiation.[1,2] The defects and color centers created by this ion implantation can be useful in technological applications[3,4] but a clear understanding of their nature and of their response to UV light is still lacking.

Variable-energy positron annihilation spectroscopy (PAS) has been shown to be an excellent technique for probing near surface defects induced by ion irradiation.[5,6] Specifically, irradiated SiO_2-based samples have been studied using PAS on several occasions.[7–11] Fujinami and Chilton[7] investigated the effect of boron implantation of SiO_2 and by a process of elimination reduced the possible positron trapping sites to a choice between the nonbridging oxygen hole center (NBOHC), peroxy radicals, and dissolved oxygen. They followed this work by studying excimer-laser-induced trapping in various types of thin SiO_2 films, proposing that the most significant positron trap was the NBOHC.[9] Khatri *et al.*[11] examined the effect of both gamma-ray and x-ray irradiation of SiO_2 films on Si substrates; they also identified the NBOHC as a strong positron trapping site. Uedono *et al.*[8] used the positron lifetime technique[5,12] to observe the effect of 5 MeV electron radiation on vitreous SiO_2. They found that the formation of positronium (the positron–electron bound state) within the bulk of the material was greatly reduced after irradiation. Hasegawa *et al.*[10] used both the positron lifetime technique and angular correlation of annihilation radiation (ACAR) to study neutron-irradiated silica glass. They also found that the probability of Ps formation decreased dramatically after irradiation, however, upon heating to ~600 °C the Ps signal returned to its preirradiation level. They proposed that in this case the neutron-irradiation-induced positron trapping sites were the E' center and the peroxy radical.

The growing body of work on SiO_2 using the PAS technique is enabling the development of a firm understanding of positron behavior in SiO_2 materials. The work presented here attempts to use the results of variable-energy PAS in conjunction with knowledge gained from previous studies to further identify positron trapping sites, to construct a depth profile of implantation-induced defects, to estimate absolute defect concentrations in Si-implanted fused silica, and to determine the annealing characteristics of the positron trapping defects. The PAS results are correlated with results of previous and ongoing optical measurements.

II. EXPERIMENT

A. Sample implantation and photobleaching

High-purity synthetic fused silica substrates (Suprasil-2, Heraeus Amersil, Inc.) were irradiated at room temperature in a vacuum of 10^{-6} Torr with 1.5 MeV Si^+ ions. The ion beam had a diameter of 3 mm and was scanned over an area of either 1 or 4 cm^2 on the sample surface. The beam current was between 10 and 30 nA, permitting uniform low-dosage implantation in the range 10^{11} to 10^{13} ions cm^{-2}. Preirradiation OH concentrations were quoted by the manufacturer to be between 900 and 1200 ppm. The samples were 0.5 mm thick and offered a surface of a few cm^2. The photobleaching of the irradiated samples was carried out using a Lumonics EX-500 excimer laser emitting 20 ns laser pulses

 0021-8979/96/79(12)/9022/7/$10.00

from an ArF gas mixture (193 nm, 6.4 eV). The energy density of the laser beam was 83 mJ cm^{-2} per pulse with 300 laser pulses delivered resulting in a total of 24 J cm^{-2}.

B. Positron annihilation spectroscopy

The University of Western Ontario slow-positron-beam facility has been described elsewhere.[13] Monoenergetic positrons in the energy range 0.3–60 keV are implanted into the sample. In penetrating the solid the positrons lose energy rapidly, thermalizing in ~10 ps. The mean depth $\overline{z}$ (Å) of implantation into the sample may be varied by changing the incident beam energy E (keV),

$$\overline{z} = (400/\rho)E^n, \tag{1}$$

where ρ is the density of the solid (g cm^{-3}) and n is a constant deduced empirically to be $n=1.6$.[14] The depth distribution of thermalized positrons is broad and asymmetric. It can be described by a Makhovian distribution,

$$P(z) = (mz^{m-1}/z_0^m)\exp[-(z/z_0)^m] \tag{2}$$

with

$$z_0 = \overline{z}/\Gamma[(1/m)+1], \tag{3}$$

where $m=2.0$.[14]

The depth at which positrons annihilate is not only determined by this broad implantation profile but also by the diffusion that occurs after the positron has thermalized. Thermal positrons diffuse in a defect-free crystalline solid for ~200 ps before annihilating. In the presence of defects the number of freely diffusing positrons decreases at a rate λ_{eff},

$$\lambda_{\text{eff}} = \lambda_f + \nu C, \tag{4}$$

where λ_f is the ''free'' annihilation rate in the bulk of the solid (4.2×10^9 s^{-1} for silica[15]), ν the specific trapping rate of the defects (s^{-1}), and C the (fractional) concentration of defects, i.e., νC represents trapping to defects. The specific trapping rate for monovacancies in silicon is 3×10^{14} s^{-1}.[16] Using these values one can estimate the limits of sensitivity of the technique: for $C=4\times10^{-7}$, 5% of positrons will be trapped, and for $C=1.5\times10^{-4}$ the number trapped becomes 95%. Positrons can be reemitted from the solid into the vacuum in the case that the surface is clean, however for the more usual case (including this study) the surface is an efficient positron trap.

Positron annihilation results in the emission of γ radiation. The 511 keV annihilation energy peak is Doppler broadened due to the momentum of the participating electrons. Generally, positrons annihilating in different electronic environments give different degrees of broadening which can be measured using high-resolution solid-state detectors.

In the present work, γ-ray spectra were collected with an intrinsic Ge detector of ~210 cm^3 volume and 1.3 keV resolution (at 511 keV), and analyzed using the S parameter, defined as the number of counts in the central region of the annihilation peak (510.27–511.73 keV) divided by the total counts in the peak (504.5–517.5 keV). The S parameter curves are then normalized by dividing the S values by the value obtained from the unirradiated bulk material. Typically, annihilation of positrons trapped by vacancy-type defects results in an increased S parameter, because the trapped positron resides further from the (repulsive) ion cores than a positron in the undefected bulk material. This results in fewer annihilations with high-momentum core electrons, reduced Doppler broadening, and a narrower annihilation line.

The S parameter versus positron energy data are analyzed using the program POSTRAP5,[17] which calculates the implantation profile and then solves the positron diffusion equation taking into account the effect of defects and electric fields. POSTRAP5 calculates, for each incident positron energy E, the fractions $F_d(E)$ of positrons which annihilate in defects, which annihilate from the freely diffusing state within the undefected bulk $F_f(E)$, and which annihilate at the surface $F_s(E)$, for a model of defects in the sample. The experimental line-shape parameter $S(E)$ can then be fitted using the equation

$$S(E) = S_s F_s(E) + S_f F_f(E) + S_d F_d(E) \tag{5}$$

where S_s, S_f, and S_d are the characteristic line-shape parameters for annihilating at the surface, in the bulk, and trapped at a defect, respectively.

In insulator materials containing large open volumes it is possible for a positron to become bound to an electron and exist in the hydrogenlike state, positronium (Ps). The singlet state (para-positronium) has a lifetime of ~125 ps and decays via two gamma rays of ~511 keV. Para-Ps decay results in a high S parameter due to the low center of mass motion of the Ps atom. The triplet state (ortho-positronium) has a much longer lifetime of ~142 ns and decays via three gamma rays with a continuous energy distribution extending from 0 to ~511 keV. The formation ratio of ortho- to para-Ps is 3:1. By monitoring the ratio of counts in the total annihilation energy spectrum compared to annihilations in the 511 keV peak only, it is possible to observe changes in the relative amount of *o*-Ps, the decay of *o*-Ps being the only positron annihilation mode producing unscattered gamma-rays with an energy less than those contained in the 511 keV photopeak. This is characterized by the R parameter, defined as[5]

$$R = (T-P)/P, \tag{6}$$

where T is the total integrated count rate in the annihilation spectrum and P is the integrated count rate of the annihilation photopeak. In practice we do not use the entire spectrum but instead use windows of 360–527 keV (total) and 490–527 keV (peak) to monitor the change in *o*-Ps formation. Discarding the spectrum below 360 keV minimizes the effect of scattered radiation on the resulting data.

When *o*-Ps exists within the bulk of a material, ''pick-off'' annihilation is highly probable as a consequence of the relatively long lifetime of *o*-Ps. In this process the positron of the *o*-Ps atom undergoes 2-γ annihilation in collision with a foreign electron having opposite spin. Therefore, although three times more *o*- than *p*-Ps is formed, the measured annihilation events resulting from *o*-Ps decay are only a small fraction of those measured from the decay of *p*-Ps. Pick-off greatly reduces the amount of 3-gamma annihilation observed from within the bulk.[12]

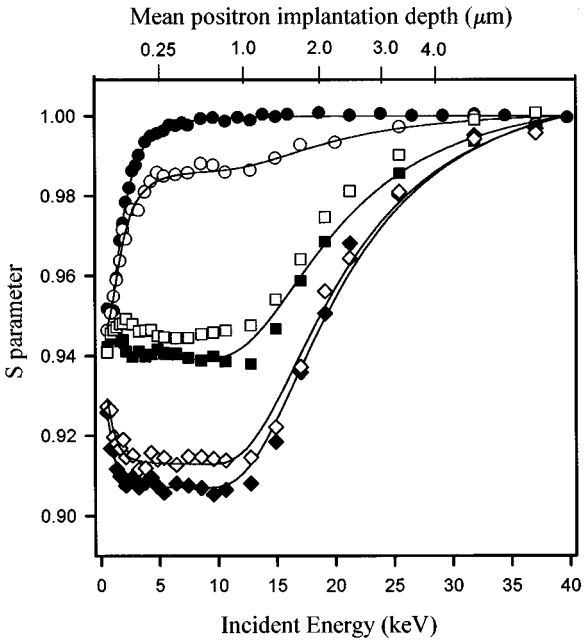

FIG. 1. *S* parameter vs positron implantation energy (and mean positron implantation depth) for silica implanted with various fluences of 1.5 MeV Si ions. The symbols denote (●) unimplanted, and implanted at fluences of (○) 1×10^{11}, (■) 1×10^{12}, (◇) 5×10^{12}, and (◆) 1×10^{13} ions cm^{-2}. Also shown (□) are data obtained from the sample implanted with a fluence of 1×10^{12} ions cm^{-2} after photobleaching with an ArF laser. Solid lines show fits to the data obtained using the program POSTRAP5.

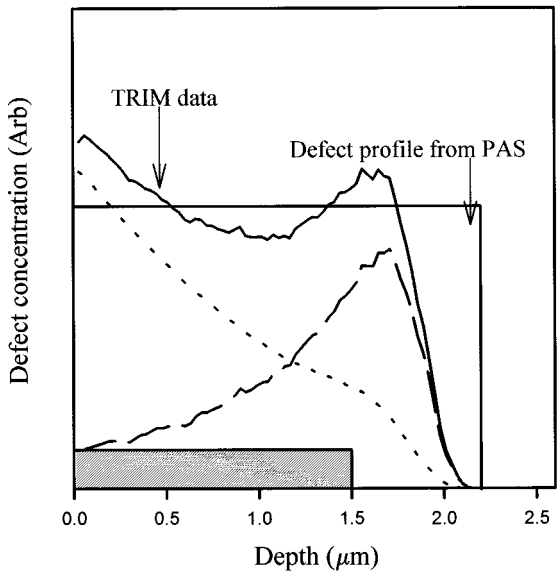

FIG. 2. The defect distribution used to model the positron data in Fig. 1 is shown as a uniform block. The distributions of electronic and nuclear stopping defect types deduced from TRIM are shown as dotted and dashed lines, respectively. The sum of the defect types is plotted as the solid line. The defect profile used to model the position data in Fig. 3 after annealing to 450 °C is shown as the shaded uniform block, normalized to the distribution used to model the data from the unannealed samples.

C. Measurements of volume compaction

One sample was irradiated to a dose of 10^{13} cm^{-2} through a steel contact mask comprising ten open rectangles thus producing alternating implanted and unimplanted regions. The height of the irradiation-induced step was measured by stylus profilometry (Dektak) and averaged over the ten steps. The measurements were carried out on the as-implanted sample and on the sample after subsequent anneals in a conventional furnace in an argon ambient.

III. RESULTS

Figure 1 shows the *S* parameter versus positron energy (and mean positron implantation depth) curves for an unirradiated silica sample and for samples irradiated with 1.5 MeV Si^+ ions to fluences of 1×10^{11}, 1×10^{12}, 5×10^{12}, and 1×10^{13} cm^{-2}. Fits to the experimental data obtained using the program POSTRAP5 (Ref. 17) are shown as solid lines. Also shown in Fig. 1 is the *S* parameter curve for the 1×10^{12} ions cm^{-2} sample after photobleaching with an ArF excimer laser.

Figure 2 shows the defect density profile predicted by the program TRIM,[18] together with the profile used to model the positron *S* parameter data. Further explanation of these profiles is given below.

Figure 3 shows the results of isochronal annealing of a sample implanted to a fluence of 1×10^{13} cm^{-2}. A fit to the data after annealing to a temperature of 450 °C is also plotted as a solid line.

Figure 4 is a plot of the % recovery compared to the value obtained for an unimplanted sample of the *S* and *R* parameters, for a positron energy of 6 keV. Also shown is the recovery of the measured step height at the boundary of

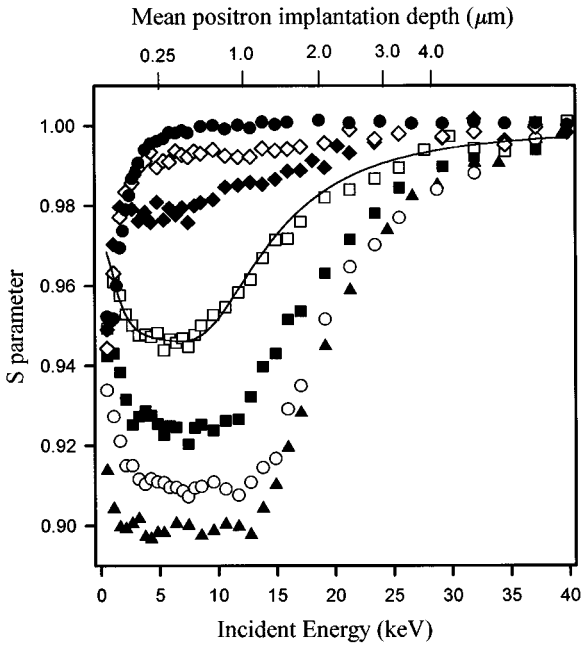

FIG. 3. *S* parameter vs positron implantation energy (and mean positron implantation depth) for a sample implanted at a fluence of (▲) 1×10^{13} ions cm^{-2}, and after annealing in isochronal stages at temperatures of (○) 350 °C, (■) 400 °C, (□) 450 °C, (◆) 500 °C, and (◇) 550 °C. Also shown (●) are equivalent data for an unimplanted sample. The data after annealing to 450 °C has been modeled using POSTRAP5, the result of which is shown as a solid line.

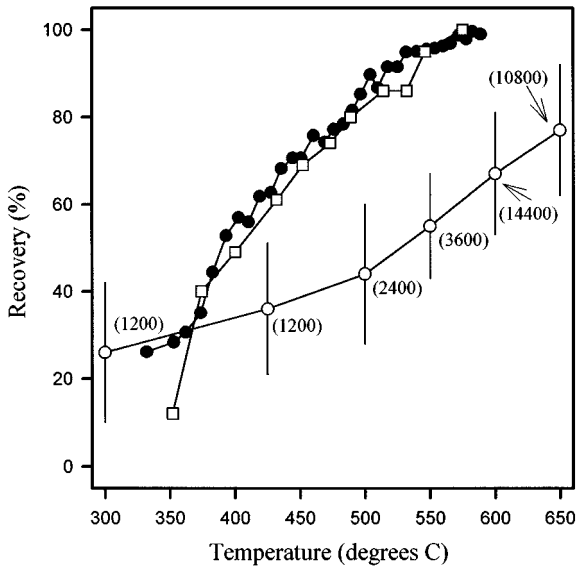

FIG. 4. Recovery toward the value obtained from the unimplanted sample vs annealing temperature for (●) S and (□) R parameters measured for a positron energy of 6 keV, and (○) step height of the boundary between implanted and unimplanted region, for a sample implanted to a fluence of 1×10^{13} ions cm^{-2}. Numbers in brackets indicate the annealing time in seconds of the sample from which step height measurements were taken. Solid lines are guides to the eye only.

the implanted region versus temperature for the same sample. The S and R parameter data were obtained over a period of 5 h of continuous ramping of the temperature. The step height data were obtained by annealing in steps, the duration of which are indicated on the plot. Consistent measurements of step height made after shorter annealing times are not shown. The R parameter data have undergone a three-point smoothing procedure.

The defect concentrations resulting from the fitting procedure performed on the data shown in Figs. 1 and 3 are summarized in Table I together with the initially-created defect concentrations and the average deposited energy density deduced from TRIM.[18]

TABLE I. Summary of data. Measured defect concentrations (cm^{-2}) from positron annihilation results, and initially created defect concentrations from TRIM are shown. The defect concentrations quoted for the sample irradiated at a fluence of 1×10^{13} cm^{-2} and marked with an asterisk are deduced from positron results after heating the sample to 450 °C. Also given is the average density of energy deposited by the ions in the implanted region.

Fluence (cm^{-2})	Defect concentration (cm^{-2}) measured by PAS	Defect production concentration (cm^{-2}) deduced from TRIM	Average deposited energy density (keV cm^{-3})	S_{imp}
1×10^{11}	3.1×10^{13}	1.2×10^{15}	7.5×10^{17}	0.986
1×10^{12}	3.1×10^{14}	1.2×10^{16}	7.5×10^{18}	0.940
5×10^{12}	1.4×10^{15}	6.0×10^{16}	3.75×10^{19}	0.914
1×10^{13}	2.8×10^{15}	1.2×10^{17}	7.5×10^{19}	0.907
1×10^{13}*	1.1×10^{14}	…	…	0.946

IV. DISCUSSION

A. *S* and *R* parameter response to Si ion implantation

The S parameter curve obtained for the unimplanted sample shown in Fig. 1 exhibits a sharp rise from the surface S value S_s of 0.945 to the normalized bulk S value S_f at an incident energy of ~8 keV. The steep rise of this curve is indicative of a short positron diffusion length L_+. In this case a value of $L_+ = 35\pm5$ nm can be deduced, which compares to a value of 19.7 ± 0.5 nm quoted by Uedono *et al.*[8] for vitreous silica. Upon irradiation with 1.5 MeV Si ions, the S parameter corresponding to the implanted region S_{imp} is observed to decrease. A saturated value for S_{imp} of 0.907 is obtained for an ion dose of 1×10^{13} cm^{-2}. This corresponds to an average deposited energy density of 7.5×10^{19} keV cm^{-3}. A similar reduction in S was observed by Fujinami and Chilton[7] for 100 keV boron-implanted SiO_2, equivalent to 2×10^{20} keV cm^{-3} of deposited energy. The shape of the S parameter curves for energies <~4 keV varies with ion fluence. This is an indication of positron diffusion from the implanted region to the sample surface. All the data were fit using the same surface parameter S_s, whereas S_{imp} varies with fluence. It should be noted that although the S parameter measured for the lowest positron energies (~400 eV) varies with implant fluence, this should not be interpreted as a change in the surface condition. The change in S at 400 eV is due to a change in the fraction of positrons able to diffuse to the surface.

A large proportion of positrons incident upon SiO_2 form the positron–electron bound state, positronium (Ps), within the bulk.[8] This has been estimated by Dannefaer and co-workers[15] to be as much as 80% for fused quartz. Decay of the short-lived singlet state, para-Ps, gives rise to a high S parameter value as a result of the relatively small center of mass momentum of the p-Ps atom. Suppression of the formation of Ps within the bulk of a sample would be expected to therefore result in a lowering of the measured S parameter. It is suggested that the ion irradiation creates defects within the material which prevent positrons from forming Ps, thus resulting in a reduced value for S_{imp}. Suppression of Ps formation has been reported in the cases of neutron, electron, and photon irradiation of SiO_2.[8–10]

This is further supported by the measurement of the 3γ annihilation R parameter value. Although almost all of the long-lived, triplet state o-Ps formed in the bulk of a solid annihilates by pick-off, resulting in 2γ annihilations, a small but detectable amount of 3γ annihilation is observed from silica. The R parameter in the present study was observed to decrease with increasing radiation dose.

B. Implantation-induced defect distribution

The S parameter versus incident positron energy data in Fig. 1 have been modeled successfully using the program POSTRAP5.[17] A value for the defect S parameter S_d was obtained from the 1×10^{13} cm^{-2} implanted sample assuming that in this case positron trapping has saturated, i.e., the concentration of defects is large enough to ensure that all positrons are trapped prior to annihilation and therefore the introduction of further trapping sites has no effect on the

measured S parameter. The results of the fitting procedure are summarized in Table I. Figure 2 shows the defect model used to generate the fits shown in Fig. 1, plotted together with a distribution of defects deduced from the ion-implantation simulation program TRIM.[18] Both require some detailed description.

The positron data could not be modeled satisfactorily using the vacancy profile generated by TRIM, which assumes that atomic displacements are created exclusively by nuclear stopping. From previous studies of irradiated silica,[8] it is, however, expected that vacancies should account for at least some of the positron trapping. Although vacancy-type defects would usually be expected to increase the S parameter above the value for the undefected bulk,[6] it has been suggested that in silica they trap positrons and thereby prevent the formation of Ps, reducing the S parameter as described above.[8]

Because the measured defect distribution does not match the vacancy distribution predicted by TRIM, the identification of further trapping sites is aided by the knowledge that they are therefore likely associated with the electronic, rather than nuclear, stopping of the implanted ions. Structural damage to SiO_2 caused by ionization can be associated with

(i) the breaking of Si—O bonds with the subsequent movement of the O away from the Si sufficiently far to prevent the bond reforming,[19]
(ii) the breaking of a strained Si—Si bond around a preexisting oxygen vacancy, or
(iii) the radiolysis of a hydroxyl group.[20]

The dominant broken-bond defects in silica are the E' center, the NBOHC, and the peroxy radical oxygen hole center (PROHC). These defects have been described in detail by Griscom.[21] The E' center is positively charged, whereas the subsequent trapping of an electron at the NBOHC results in the creation of a negatively charged defect of the form $\equiv$Si–O–. Therefore, the NBOHC would be expected to trap positrons with far greater efficiency than the E' center. The suggestion that the NBOHC acts as a positron trapping site has been used to explain the variation in Ps suppression among SiO_2 samples containing varying concentrations of OH impurities.[8] The Ps formation probability for synthesized vitreous SiO_2 specimens with OH concentrations <5 ppm was found to be lower than that for one with an OH concentration of <200 ppm. Kerwin and Galeener[22] have shown that the creation of E' centers due to x-ray irradiation increases linearly with radiation dose for OH$\approx$1200 ppm and nonlinearly for OH$\approx$4 ppm. The increased relative growth of the E' center in the low OH concentration sample was attributed to the abundance of preexisting E' centers which merely require activating by irradiation. These preexisting defects are thought to be suppressed by OH groups. The authors suggested that this idea may be extended to include the NBOHC. Alternatively, the creation of such defects by the radiolysis of a hydroxyl group may result in the concentration of NBOHCs being directly dependent on the concentration of OH.

The samples in the present study contained concentrations of OH groups between 900 and 1200 ppm. Although all of the spectra in Fig. 1 were obtained from equivalent starting material and hence contain the same concentration of OH impurities, the sample implanted with a dose of 1×10^{13} cm^{-2} shown in Fig. 3 originated from an alternative batch. The difference in S_{imp} between the two 1×10^{13} cm^{-2} samples in Figs. 1 and 3 can therefore be attributed to differing concentrations of OH groups in the preimplanted material.

Figure 1 also shows the effect of photobleaching on the value of S_{imp} for the 1×10^{12} cm^{-2} sample. A similar response for all postimplantation photobleaching was observed, however, only that for the 1×10^{12} cm^{-2} sample is shown to maintain clarity. The effect of a small increase of S_{imp} shows that the photobleaching has relatively little effect on positron trapping. Albert *et al.*[23] showed that bleaching of irradiated silica with a KrF excimer laser significantly reduced the optical absorption B_2 band, associated with a single oxygen vacancy. Furthermore, evidence that ArF excimer laser bleaching is more efficient than KrF has been shown.[1] The single oxygen vacancy can therefore be eliminated as an efficient positron trapping site relative to other sites created by the ion implantation. In the same study[1] it was found that the E' band exhibited a remarkable resistance to bleaching. It has also been observed in preliminary photoluminescence studies that both the NBOHC-related 1.9 eV photoluminescence band[24,25] and the 4.8 eV absorption band associated with $\equiv$Si–O$_-$ (Ref. 26) are persistent and remain present when the samples have received 24 J cm^{-2} of 6.4 eV photons.[27]

The defect profile used to model the S parameter data in Fig. 1 can be explained in terms of two defect types, the first resulting from the ionizing effects of the Si ion implantation and most likely associated with oxygen hole centers with or without trapped electrons, and the second a result of vacancy-type defects caused by nuclear stopping of the incident ions. These two types of defects have been identified as trapping sites for positrons in 100 keV boron-irradiated thermally grown SiO_2.[7]

The model assumes a uniform distribution of defects (shown schematically in Fig. 2) assigned an arbitrary trapping rate of 3×10^{14} s^{-1} [i.e., the trapping rate for point defects in Si (Refs. 16, 28] extending to a depth of 2.2 μm. It is clear from the shape of the defect profile required to model the positron data that it is necessary to include in the model a contribution from electronic stopping. In order to obtain a profile of defect density versus depth it is necessary to assume a value for the energy lost via electronic stopping per defect created: We have assumed an average of 30 eV is expended in each ionization event,[29] and that seven events cause the creation of one positron trapping site associated with a NBOHC. The electronic stopping defects, summed with the monovacancies (electronic plus nuclear contributions), result in a defect profile which resembles that required to model the positron data.

The growth of the defect concentration up to a dose of 5×10^{12} cm^{-2} is seen to be approximately linear, i.e., newly implanted ions form the same number of stable defects as previously implanted ions, with no interaction between defects produced by different ions. This is in contrast to the

sublinear growth of defects observed by Nielsen *et al.*[30] using PAS, for Si ion-implanted *p*-type Si(100) in the same dose range; however, Simpson *et al.* found the growth of defects in ion-implanted Si(100) to be linear up to a fluence of 10^{12} cm^{-2}.[31] The absolute defect concentrations obtained from fitting of the PAS data are ~40 times less than the concentration of defects predicted by TRIM. An identical comparison of defect concentrations obtained from PAS and TRIM by Simpson *et al.*[31] found that the concentrations obtained from PAS were an order of magnitude less than those from TRIM. This apparent discrepancy can be explained by the recombination of defects after their initial creation, which is not accounted for by TRIM.

The reduction of Ps following ion irradiation (due to the trapping of positrons in radiation-induced defects) forms the basis from which the defect concentrations in Table I are calculated. It is noted that the fitting procedure used in this study ignored the existence of defects in the silica prior to implantation; however, the model in this case is still applicable. If one assumes that there are two defect states (one corresponding to ion implantation-induced defects and the other to preexisting defects prior to implantation), the total trapped fraction is given by

$$F=(\nu_1 C_1+\nu_2 C_2)/(\lambda_f+\nu_1 C_1+\nu_2 C_2), \tag{7}$$

where F is the total trapped fraction, ν_1 and ν_2 are the trapping rates for positrons into ion-induced defects and preexisting defects, respectively, C_1 and C_2 are the defect concentrations, and λ_f is the annihilation rate (1/lifetime) of freely diffusing positrons in the sample. By ignoring the presence of preexisting defects (a necessary approximation in this study), it can be seen from Eq. (7) that an artificially large value of C_1 could be obtained. This problem may be offset by increasing the value of λ_f in Eq. (7). It is noted that the depth and shape of the defect profile used are not affected by this—only the absolute concentrations are affected.

C. Volume compaction

Volume change in the implanted samples was measured by profiling the surface height discontinuity at the boundary of an area masked during implantation. For the 1×10^{13} cm^{-2} sample a step height of 20 ± 2 nm was measured. The compaction of silica under irradiation has been well documented.[19,29,32,33] Eernisse and Norris[19] showed that for 500 keV Ar-implanted silica the compaction increased with fluence up to a value of $\sim1\times10^{14}$ cm^{-2} equivalent to a deposited energy density of 5×10^{20} keV cm^{-3}, and then saturated. They were also able to separate compaction resulting from ionization and from atomic collisions (i.e., displacement). Compaction due to the atomic collisions was found to be ~200× greater than that for ionization, for a given ion energy. The ionization-induced compaction was consistent with broken Si—O bonds and therefore the formation of NBOHCs. It should be noted that radiation-induced compaction results in the closing of free space within the bulk of the silica, which can be expected to contribute to the suppression of Ps.

D. Heating effects

The results of isochronal annealing of a sample implanted to a fluence of 1×10^{13} cm^{-2} are shown in Fig. 3 and are similar to those obtained for thermally grown SiO_2 by Fujinami and Chilton.[7] Annealing effects are observed at 350 °C and complete recovery of the unimplanted *S* parameter spectrum is observed at 600 °C. At 450 °C a change in the shape of the spectrum is observed compared to that for lower temperatures. The recovery of the end-of-range defects appears to be faster than that for the defect region nearer the surface. The *S* parameter curve for the sample annealed at 450 °C has been modeled assuming complete recovery of the defect region from 1.5 μm below the surface and only partial recovery of the defect region up to 1.5 μm. This model is shown as the shaded block in Fig. 2. The distribution of defects caused by atomic collisions is peaked at ~1.7 μm, whereas defects associated with electronic stopping are found in greater concentrations closer to the surface. This may be an indication that the vacancy-type defects anneal at a faster rate than those resulting from broken-bonds.

Griscom[21] pointed out that a diversity of production and annealing kinetics for irradiated SiO_2 samples exist, depending on the character of the irradiation and the water content and thermal history of the sample. An annealing temperature of around 600 °C for NBOHCs is consistent with previous results.[21] Also, Dannefaer and co-workers[15] reported that the recovery of mono- and divacancies in synthetic αSiO_2 begins at around 300 °C.

The structural recovery of the sample is indicated by the decrease in step height at the boundary of the implanted region with increasing temperature. Figure 4 shows the % recovery of step height versus temperature. Following an anneal at 650 °C the step height was decreased to 5 ± 1 nm, from 20 ± 2 nm observed after irradiation. This reduction confirms the annealing of structural defects and is consistent with previous results.[19] Also shown in Fig. 4 is the % recovery of both the *S* and *R* parameters measured for an incident energy of 6 keV. These measurements were made as the temperature was ramped over a 5 h period in contrast to the measurement of step height which was made in discrete steps. A clear correlation is observed between the *S* and *R* parameters confirming the *S* parameter dependence on Ps suppression.

V. CONCLUSIONS

Si ion implantation-induced defects in fused silica have been probed using a variable-energy positron beam. The *S* parameter for the implanted region was lower than that for the unimplanted, and decreased with increasing radiation fluence. A saturated value of $S\sim0.91$ was observed for a fluence of 1×10^{13} cm^{-2}. The reduction in the measured *S* parameter value is associated with the suppression of Ps formation resulting from the trapping of positrons by radiation-induced defects. The defect distribution used to model the *S* parameter data encompasses two distinct defect types in the implanted material: nonbridging oxygen hole centers caused by the electronic stopping of the ions and subsequent breaking of bonds; and open volume defects

(probably divacancies) caused by the nuclear stopping. Volume compaction of the implanted material was observed by monitoring the step height at the boundary of the implanted and unimplanted regions. Complete recovery of the unimplanted *S* parameter spectrum was observed after annealing the sample at a temperature of 600 °C, with the vacancy-type defects annealing at a faster rate than the NBOHCs. A reduction of 75% in the step height was also observed after annealing at 650 °C. Work is in progress to study samples that have been implanted at higher and lower incident ion energies, from which it should be possible to probe separately the defects due to electronic and nuclear stopping of the ions, respectively.

ACKNOWLEDGMENT

The authors would like to acknowledge A. Tchebotareva for assistance with the profilometry measurements.

[1] M. Verhaegen, L. B. Allard, J. L. Brebner, M. Essid, S. Roorda, and J. Albert, Nucl. Instrum. Methods B (to be published).
[2] J. Albert, K. O. Hill, B. Malo, D. C. Johnson, J. L. Brebner, Y. B. Trudeau, and G. Kajrys, Appl. Phys. Lett. **60**, 148 (1992).
[3] V. Mizrahi, P. J. Lemaire, T. Erdogan, W. A. Reed, D. J. DiGiovanni, and R. M. Atkins, Appl. Phys. Lett. **63**, 1727 (1993).
[4] B. Malo, F. Bilodeau, J. Albert, D. C. Johnson, K. O. Hill, Y. Hibino, and M. Abe, Proc. SPIE **2044**, 42 (1993).
[5] P. J. Schultz and K. G. Lynn, Rev. Mod. Phys. **60**, 701 (1988).
[6] P. Asoka-Kumar, K. G. Lynn, and D. O. Welch, J. Appl. Phys. **76**, 4935 (1994).
[7] M. Fujinami and N. B. Chilton, Appl. Phys. Lett. **62**, 1131 (1993).
[8] A. Uedono, T. Kawano, S. Tanigawa, and H. Itoh, J. Phys. Condens. Matter **6**, 8669 (1994).
[9] M. Fujinami and N. B. Chilton, Appl. Phys. Lett. **64**, 2806 (1994).
[10] M. Hasegawa, M. Tabata, T. Miyamoto, Y. Nagashima, T. Hyodo, M. Fujinami, and S. Yamaguchi, Mater. Sci. Forum **175–178**, 269 (1995).
[11] R. Khatri, P. Asoka-Kuma, B. Nielsen, L. O. Roellig, and K. G. Lynn, Appl. Phys. Lett. **63**, 385 (1993).
[12] P. Hautojärvi and A. Vehanen, in *Positrons in Solids*, edited by P. Hautojärvi (Springer, Berlin, 1979).
[13] P. J. Schultz, Nucl. Instrum. Methods B **30**, 94 (1988).
[14] S. Valkealahti and R. M. Nieminen, Appl. Phys. A **35**, 51 (1984).
[15] S. Dannefaer, T. Bretagnon, and D. Kerr, J. Appl. Phys. **74**, 885 (1993).
[16] S. Dannefaer, Phys. Status Solidi A **102**, 481 (1987).
[17] G. C. Aers, in *Positron Beams for Solids and Surfaces*, The Proceedings of the Fourth International Workshop, edited by P. J. Schultz, G. R. Massoumi, and P. J. Simpson, AIP Conference Proceedings 218 (AIP, New York, 1991).
[18] J. F. Ziegler, J. P. Biersack, and U. Littmark, *The Stopping and Range of Ions in Solids* (Pergamon, New York, 1985).
[19] E. P. Eernisse and C. B. Norris, J. Appl. Phys. **45**, 5196 (1974).
[20] D. L. Griscom, Nucl. Instrum. Methods B **1**, 481 (1984).
[21] D. L. Griscom, J. Non-Cryst. Solids **73**, 51 (1985).
[22] D. B. Kerwin and F. L. Galeener, Phys. Rev. Lett. **68**, 3208 (1992).
[23] J. Albert, B. Malo, K. O. Hill, D. C. Johnson, J. L. Brebner, and R. Leonelli, Opt. Lett. **17**, 1652 (1992).
[24] L. N. Skuja and A. R. Silin, Phys. Status Solidi A **56**, K11 (1979).
[25] J. H. Stathis and M. A. Kastner, Philos. Mag. **49**, 357 (1984).
[26] S. Munekuni, T. Yamanaka, Y. Shimogaichi, R. Tohmon, Y. Ohki, K. Nagasawa, and Y. Hama, J. Appl. Phys. **68**, 1212 (1990).
[27] L. B. Allard and J. L. Brebner (unpublished).
[28] P. Mascher, S. Dannefaer, and D. Kerr, Phys. Rev. B **40**, 11 764 (1989).
[29] W. Primak and R. Kampwith, J. Appl. Phys. **39**, 5651 (1968).
[30] B. Nielsen, O. W. Holland, T. C. Leung, and K. G. Lynn, J. Appl. Phys. **74**, 1636 (1993).
[31] P. J. Simpson, M. Vos, I. V. Mitchell, C. Wu, and P. J. Schultz, Phys. Rev. B **44**, 12 180 (1991).
[32] E. P. Eernisse, J. Appl. Phys. **45**, 167 (1974).
[33] T. A. Dellin, D. A. Tichenor, and E. H. Barsis, J. Appl. Phys. **48**, 1131 (1977).